RSCAM Group Project Six

Efficient Molecular Dynamics with High Accuracy

Karolína Benková, Emily McClung, Danner Morrison, and Yichen Su.

Abstract

There exist numerous numerical integration methods for solving the Hamiltonian systems modeling molecular dynamics. Although energy is a conserved quantity of a Hamiltonian system that is not conserved exactly during discretization, symplectic integrators are accurate to some order with respect to preserving energy invariance. A prominent symplectic integrator, the Störmer-Verlet method, is conventionally applied towards molecular dynamics problems, but has a relatively low (second) order of accuracy. This report is concerned with making comparisons with this method to other numerical integration schemes for solving Hamiltonian systems: the Takahashi-Imada integrator and its simplified non-symplectic version, along with the Suzuki-Yoshida method. The first two methods are second order but can achieve effective order four, whereas the last method is fourth order. We evaluate these methods based on their performance, stability, and computational cost relative to each other and the Störmer-Verlet method. They are applied to a variety of problems with increasingly complex Hamiltonians. We found that higher order methods must sacrifice either accuracy or computational cost for complicated systems, such as a 12 particle system we modeled. However, the simplified Takahashi-Imada method appears to balance both in a way that could make it effective for such a system. We also found that, although the Yoshida method achieves consistent results, it requires three force evaluations, resulting in a disadvantageous computational cost by comparison.

Sections

Introduction

Numerical integration schemes are heavily relied upon to solve the systems of differential equations underpinning problems in a variety of disciplines. The mechanics underlying many molecular dynamics problems rely on the solutions of Hamilton's equations. Not all integrators are suitable for Hamiltonian systems, however. Energy is a conserved quantity in these dynamical systems, being held constant along the solution curves that describe the trajectories of the molecules. This conservation does not occur during discretization. Conventional numerical integrators, such as Euler's Method, may yield errors in energy which grow exponentially with time. Their lack of stability makes these numerical methods unsuitable for long-term simulation.

This shortcoming is addressed by the implementation of specific subclasses of geometric integrators, which preserve the geometric properties characteristic to Hamiltonian flow maps [5]. Although energy cannot be conserved by these methods, they are perturbed energy invariant. One such integration scheme, Störmer-Verlet method, has frequently been the choice for the simulation of molecular dynamics. It is known for its good numerical stability, along with possessing the desirable properties of being symmetric, time-reversible, symplectic, and volume-preserving. However, it has a low order of accuracy with regards to calculating trajectories [4]. Therefore, high-order integration methods may prove to be more desirable.

The aim of this paper is to compare different numerical integration schemes with the more conventionally implemented Störmer-Verlet and Euler methods, while considering each of their respective trade-offs. We briefly overview the fundamentals of Hamiltonian dynamical systems in Section 1, where we also establish the notation we will use throughout the report, and discuss the types of numerical methods that preserve geometric properties of the flow of these systems. In Section 2, we summarize the numerical methods. In addition to the aforementioned Störmer-Verlet method, which is of second order, we compare it with the Takahashi-Imada integrator, along with the simplified version of that method, both of which are of effective order four. The last method we introduce is the Suzuki-Yoshida method, which is a fourth order schemed derived from the Störmer-Verlet method. In Section 3, we investigate the stability of these methods with a simple harmonic oscillator system example. We apply the methods to a variety of systems of increasing complexity in Section 4: a harmonic oscillator, an unsymmetric pendulum, both a single and double spring pendulum system, a trimer model, and finally, a 12-atom system. Finally, in Section 5 we conclude this paper by evaluating the performance and difference (both in theory and through experimentation) to determine whether higher order numerical integration schemes are justified to implement in practical experiments over the Störmer-Verlet method.

The figures illustrating the results from our numerical experiments, and the relevant code, can be found in the Appendix, with details on the coefficients used in the 12-atom system, along with our derivations for the stability of each method on the simple harmonic oscillator example.

1 Preliminaries

1.1 Hamiltonian Dynamical Systems

We can model a molecular dynamics problem in terms of the trajectories of the involved particles as a dynamical system governed by Hamilton's equations. In general, by framing this problem as a system of N-many bodies in three dimensions with individual trajectories and inter-particle interactions, the resulting Hamiltonian is

$$H(\mathbf{q},\mathbf{p}) = \frac{1}{2}\mathbf{p}^\top \mathbf{M}^{-1}\mathbf{p} + U(\mathbf{q}), \tag{1}$$

where $\mathbf{M}$ is a $3N\times 3N$ positive definite diagonal mass matrix [5], $\mathbf{q} = (\mathbf{q_1}, \mathbf{q_2}, \ldots, \mathbf{q_N})$ is a $3N$-dimensional vector representing the position $\mathbf{q_j} = (q_{1,j}, q_{2,j}, q_{3,j})$ of each body. Similarly, $\mathbf{p} = (\mathbf{p_1}, \mathbf{p_2}, \ldots, \mathbf{p_N})$ is a $3N$-

dimensional vector representing the momentum $\mathbf{p_j} = (p_{1,j}, p_{2,j}, p_{3,j})$ of each body in canonical coordinates. The function $U(\mathbf{q})$ is the potential function [1]. The dynamical system can be simplified easily to two dimensions, or extended to higher dimensions.

If we denote $\mathbf{r} = (\mathbf{q}, \mathbf{p})$ as the state of the system, then the system of differential equations that governs the evolution of the Hamiltonian system is

$$\dot{\mathbf{r}} = \begin{bmatrix} \dot{\mathbf{q}} & \dot{\mathbf{p}} \end{bmatrix}^\top = \mathbf{J} \cdot \nabla \mathbf{H}(\mathbf{q},\, \mathbf{p}) = \mathbf{f}(\mathbf{r}), \text{ with } \mathbf{J} = \begin{bmatrix} 0 & \mathbf{I} \\ -\mathbf{I} & 0 \end{bmatrix}. \tag{2}$$

Here $\mathbf{I}$ is the identity matrix corresponding to the dimension of either $\mathbf{q}$ or $\mathbf{p}$. Given the complexity of the Hamiltonians we encounter in molecular dynamics, it can prove prohibitive or impossible to analytically solve the equations of motion underpinning the trajectories of these many interacting bodies. Not all numerical methods are suitable for the task, however.

An important property of the Hamiltonian is the conservation of energy. If Eq.(1) for a given system doesn't possess an explicit dependent on time (i.e. $H(\mathbf{q}, \mathbf{p}, t)) = H(\mathbf{q}, \mathbf{p})$, then the system is time-invariant (i.e. $\dot{H} = 0$). A concern with some numerical methods is undesirable energy drift. An advantage of symplectic integrators is that Hamiltonian will remain slightly perturbed from the original, which is beneficial when studying the long-term simulation of molecular dynamics [3].

1.2 Geometric Integrators

Let $\mathscr{S}(t)$ be the set of points in the phase space associated with Eq. (2) and described by the flow map $\phi_t(\mathscr{S}(0)) = \mathscr{S}(t)$. According to Liouville's Thereom, since the divergence of Eq. (2) is 0 (i.e. $\nabla \cdot \mathbf{f}(\mathbf{r}) = 0$), then the volume of $\mathscr{S}(t)$ is invariant with respect to t. As a result, all Hamiltonian systems have volume preserving flows [1].

An ideal numerical scheme would be a geometric integrator which, among other properties, reproduces this geometric characteristic of a Hamiltonian system. Suppose we define a numerical flow $\Phi_h : (\mathbf{q_n}, \mathbf{p_n}) \mapsto (\mathbf{q_{n+1}}, \mathbf{p_{n+1}})$ related to such a numerical scheme. If $\det(\Phi_h') = 1$, then this map reproduces this geometric property [1].

1.3 Symplectic Integrators

Another prominent geometric characteristic of Hamiltonian systems is symplecticity. Given the flow $\phi_t(\mathbf{r})$, the derivative $\phi_t' = \nabla_{\mathbf{r}} \phi_t$ should satisfy the relationship

$$\phi_t'(\mathbf{r})^T \mathbf{J}\, \phi_t'(\mathbf{r}) = \mathbf{J}, \tag{3}$$

for all $\mathbf{r} = (\mathbf{q}, \mathbf{p})$ and t where $\phi_t(\mathbf{r})$ is defined. We can reproduce symplecticity in a numerical scheme if the numerical flow $\Phi_h(\mathbf{q}, \mathbf{p})$ satisfies the relationship:

$$\Phi_h'(\mathbf{q}_n, \mathbf{p}_n)^T \mathbf{J}\, \Phi_h'(\mathbf{q}_n, \mathbf{p}_n) = \mathbf{J} \tag{4}$$

for all $(\mathbf{q}, \mathbf{p})$ and all step sizes h [5]. Note that all symplectic integrators are a subclass of geometric integrators with volume preserving flows, so it is sufficient for our numerical scheme to be symplectic to attain all of the aforementioned properties.

2 Numerical Schemes

The main motivation in designing new numerical schemes to solve Hamiltonian systems is to obtain an accurate solution in terms of the energy conservation. It is generally accepted that symplectic integrators are suitable for solving this type of problems, especially in molecular dynamics, where not all the details in the solution are necessary [3]. Methods of fourth order are said to be the most efficient, however, second order methods are often used because of their simplicity.

Ever since the concept of effective order was presented [6], it has been widely used in practice [7]. It exploits the idea of conjugacy via a homeomorphism χ_h (a change of variables), which helps to eliminate the leading terms in the expansion of the scheme's local error [1]. If there exists χ_h for numerical schemes $\mathcal{G}_h$ of order r, $\widetilde{\mathcal{G}}_h$ of order s ($s < r$), such that $\mathcal{G}_h = \chi_h^{-1}\widetilde{\mathcal{G}}_h\chi_h$, we say that the method $\widetilde{\mathcal{G}}_h$ bears an effective order r. The processing is done by first taking the initial condition z_0 and pre-processing it to $\widetilde{\mathbf{z}}_0 = \chi_h(\mathbf{z}_0)$, then taking a number of time steps with the method $\widetilde{\mathcal{G}}_h$ and post-process the result by χ_h^{-1}. The main reason to use processing is to uncover the true accuracy of the scheme by keeping only the not removable error. However, the processing serves for the purpose of deriving the effective order of a method only, and in general the method can be used with little or no processing [3].

In the next part of this section we will introduce some of the methods and their properties.

2.1 Störmer-Verlet Method

The Störmer-Verlet method, one of the most recognized and commonly used numerical integration schemes in molecular dynamics, is

$$\begin{aligned} \mathbf{p}_{n+\frac{1}{2}} &= \mathbf{p}_n - \tfrac{h}{2}\nabla\mathbf{U}(\mathbf{q}_n), \\ \mathbf{q}_{n+1} &= \mathbf{q}_n + h\,\mathbf{M}^{-1}\mathbf{p}_{n+\frac{1}{2}}, \\ \mathbf{p}_{n+1} &= \mathbf{p}_{n+\frac{1}{2}} - \tfrac{h}{2}\nabla\mathbf{U}(\mathbf{q}_{n+1}). \end{aligned} \tag{5}$$

The Störmer-Verlet method's suitability for the long-term simulation of Hamiltonian dynamical systems is due to the properties it has as a geometric integrator: the method is symmetric, reversible, volume-preserving, and symplectic [4]. Its global error in both calculating the trajectory and the energy is of order two, with no significant additional cost compared to the first order Euler's method. It also benefits from the First Same As Last (FSAL) property: the force evaluation in the last stage of the scheme is reused in the first stage of the next iteration. As a consequence, the method needs in total one force evaluation per step. Overall, due to its simplicity and low computational cost, the Störmer-Verlet method is a good comparison for other numerical integration schemes. We will use it as a measure against the other methods in this paper.

2.2 Takahashi-Imada Integrator

Although the second order Störmer-Verlet method is frequently used because of its simplicity and low computational cost, it is worth considering higher order schemes. The Takahasi-Imada Integrator (also known as Rowlands' method - *cf.* [8, 2]) is

$$\begin{aligned} \mathbf{p}_{n+\frac{1}{2}} &= \mathbf{p}_n - \tfrac{h}{2}\left(\mathbf{I} - \alpha h^2\nabla^{\mathbf{2}}\mathbf{U}(\mathbf{q}_n)\right)\nabla\mathbf{U}(\mathbf{q}_n), \\ \mathbf{q}_{n+1} &= \mathbf{q}_n + h\,\mathbf{M}^{-1}\mathbf{p}_{n+\frac{1}{2}}, \\ \mathbf{p}_{n+1} &= \mathbf{p}_{n+\frac{1}{2}} - \tfrac{h}{2}\left(\mathbf{I} - \alpha h^2\nabla^2 U(\mathbf{q}_{n+1})\right)\nabla\mathbf{U}(\mathbf{q}_{n+1}), \end{aligned} \tag{6}$$

where $\alpha = \frac{1}{12}$. This numerical scheme can be interpreted as applying the Störmer-Verlet method applied to a perturbed Hamiltonian system with a potential function $\widetilde{U}(\mathbf{q}) = U(\mathbf{q}) - \frac{\alpha}{2}h^2\|\nabla\mathbf{U}(\mathbf{q})\|^2$. As a result, the Takahashi Imada integrator is also symmetric, reversible, volume preserving, and symplectic. It is of classical order two; however, when $\alpha = \frac{1}{12}$, there exists a mapping $\chi_h : (\mathbf{p}_n, \mathbf{q}_n) \mapsto (\mathbf{p}_{n+1}, \mathbf{q}_{n+1})$ such that the method is conjugate to a fourth order method, making it effective order four [4].

The evaluation of the Hessian of the potential in Eq. (6) results in a higher order accuracy with regards to energy conservation over Störmer-Verlet method. However, this same evaluation comes with increased computational cost. It was shown in [3] that the Hessian-vector product for an N-body problem with 2-body interactions (such as the Lennard-Jones potential) can be computed at a cost of less than or equal to the cost of one force evaluation. Similarly, just like the Störmer-Verlet method, it also benefits from the FSAL property. As a consequence, the Takahashi-Imada integrator needs the equivalent of two force evaluations per step.

2.3 Simplified Takahashi-Imada Integrator

As noted in the previous section, the Takahashi-Imada integrator requires the evaluation of the Hessian of the potential function. For 2-body interactions in N-body problems, the Hessian-vector product computation is possible at a cost of one force evaluation. However, for problems involving additional interactions, the computational cost may increase. To avoid the Hessian evaluation, we can replace $\left(\mathbf{I} - \alpha h^2 \nabla^{\mathbf{2}}\mathbf{U}(\mathbf{q})\right)\nabla\mathbf{U}(\mathbf{q})$ with $\nabla\mathbf{U}(\mathbf{q} - \alpha h^2 \nabla\mathbf{U}(\mathbf{q}))$, yielding a new (simplified) scheme

$$\begin{aligned}
\mathbf{p}_{n+\frac{1}{2}} &= \mathbf{p}_n - \tfrac{h}{2}\nabla\mathbf{U}\left(\mathbf{q}_n - \alpha h^2 \nabla\mathbf{U}(\mathbf{q}_n)\right), \\
\mathbf{q}_{n+1} &= \mathbf{q}_n + h\,\mathbf{M}^{-1}\mathbf{p}_{n+\frac{1}{2}}, \\
\mathbf{p}_{n+1} &= \mathbf{p}_{n+\frac{1}{2}} - \tfrac{h}{2}\nabla\mathbf{U}\left(\mathbf{q}_{n+1} - \alpha h^2 \nabla\mathbf{U}(\mathbf{q}_{n+1})\right)
\end{aligned} \tag{7}$$

which is a $\mathcal{O}(h^5)$ perturbation of Eq. (6). This modified integration scheme is still symmetric, reversible, and of effective order four, but it is only symplectic for problems with one degree of freedom [4, 7].

Although the simplified Takahashi-Imada integrator is not (typically) symplectic, we are still interested in its use because it is computationally cheaper than other symplectic integrators of (effective) order four. Due to its FSAL property, it only requires two force evaluation and no Hessian-vector product computation, which results in an attractive trade-off.

2.4 Suzuki-Yoshida Method

Yoshida composed a method to create symplectic numerical schemes of arbitrarily high order. Since Yoshida's work is related to methods suggested by Suzuki, the method bears the name of both [1]. Taking an even-ordered symplectic method of order $2s$ for $s \geq 1$, we can iterate the scheme three times using different step sizes to make a method of order $2s + 2$. The first iteration is done using step size $\tau_0\, h$, followed by a second iteration with step size $\tau_1\, h$, after which a final iteration is performed with step size $\tau_0\, h$. If the constants τ_0, τ_1 are chosen such that $2\tau_0 + \tau_1 = 1$, the result of the final iteration yields the momentum and trajectory at time $n + 1$. The optimal values for τ_0, τ_1 are $t_0 = \frac{1}{2-\kappa}$ and $\tau_1 = -\frac{\kappa}{2-\kappa}$, where $\kappa^{2s+1} = 1$.

We can take a simple second order method, like the Störmer-Verlet method, as the base for the Suzuki-Yoshida method. Since $s = 1$, we arrive at $\tau_0 = \frac{1}{2-\sqrt[3]{2}}$ and $\tau_1 = -\frac{\sqrt[3]{2}}{2-\sqrt[3]{2}}$ for our scheme. Following the

procedure outlined in the previous paragraph, we derive the following scheme

$$\begin{aligned}\left(\mathbf{q}_{n+\frac{1}{3}}, \mathbf{p}_{n+\frac{1}{3}}\right) &= \text{Verlet}(\mathbf{q}_n, \mathbf{p}_n, \tau_0\, h),\\ \left(\mathbf{q}_{n+\frac{2}{3}}, \mathbf{p}_{n+\frac{2}{3}}\right) &= \text{Verlet}(\mathbf{q}_{n+\frac{1}{3}}, \mathbf{p}_{n+\frac{1}{3}}, \tau_1\, h),\\ \left(\mathbf{q}_{n+1}, \mathbf{p}_{n+1}\right) &= \text{Verlet}(\mathbf{q}_{n+\frac{2}{3}}, \mathbf{p}_{n+\frac{2}{3}}, \tau_1\, h).\end{aligned} \tag{8}$$

Since the Störmer-Verlet method needs one force evaluation per step and is applied three times, this fourth order Suzuki-Yoshida scheme requires three force evaluation. This makes it the method with the highest computational cost that we are considering in this report. It is noteworthy, however, that even higher order symplectic methods can be constructed by applying Suzuki-Yoshida method recursively.

3 The Stability of Numerical Methods on a Harmonic Oscillator System

Stability is a desirable property in a numerical method. For a linear Hamiltonian system, we can analyze the stability of a given method by analyzing the eigenvalues of the scheme in matrix-multiplication form. If all of the eigenvalues lie on the unit circle in the complex plane, we can conclude that the corresponding numerical method is stable [9].

To demonstrate the stability of the symplectic integrators considered so far, we will perform stability analysis on a Hamiltonian system with a simple harmonic oscillator potential (i.e. $U(\mathbf{q}) = \frac{1}{2}\omega^2\mathbf{q}^2$). This will give us insight into the dynamic behavior of the methods on a simple system and the maximal time step h.

3.1 Störmer-Verlet method

When $h < \frac{2}{\omega} \equiv \bar{h}$, the eigenvalues of the linearization of the scheme are imaginary and have a magnitude of 1 (see App. C.1). This means that for $h < \bar{h}$, the Störmer-Verlet method is stable for the harmonic oscillator system.

The method has a recursion $\mathbf{q}_{n+1} - (2 - (\omega h)^2)\mathbf{q}_n + \mathbf{q}_{n+1} = 0$, which is also found to be stable if and only for $h < \bar{h}$. The discrete energy is

$$\mathbf{p}_n^2 + (1 - (\omega h)^2/4)\omega^2\mathbf{q}_n^2 = \text{Const}, \tag{9}$$

which yields a maximal relative error in the Hamiltonian equal to $(\omega h)^2/(4 - (\omega h)^2)$, which is attained when $\mathbf{p}_n - 0$. This error behaves like $\mathcal{O}(h^2)$ for sufficiently small h, but approaches infinity as $h \to \bar{h}$ [4].

3.2 Takahashi-Imada Integrator

When $h < \frac{2}{\omega\sqrt{\alpha}} \equiv \bar{h}$, the eigenvalues $\lambda_{1,2}$ of the linearization of the scheme are imaginary and have a magnitude of 1 (see App. C.2). This means that for $h \leq \bar{h}$, the Takahashi-Imada Integrator is stable for the harmonic oscillator system. We are interested in applying this method with $\alpha = 1/12$, which would make $\bar{h} = \frac{2\sqrt{3}}{\omega}$.

The method has a recursion $\mathbf{q}_{n+1} - (2 - (\omega h)^2 + \frac{1}{12}(\omega h)^4)\mathbf{q}_n + \mathbf{q}_{n-1} = 0$, which is also found to be stable if and only if $h < \bar{h}$. The discrete energy is

$$\mathbf{p}_n^2 + \left(1 - \beta\frac{(\omega h)^2}{4}\right)\beta\omega^2\mathbf{q}_n^2 = \text{Const}, \quad \text{with } \beta = 1 - \frac{(\omega h)^2}{12}. \tag{10}$$

When we consider transformation of variables $\hat{\mathbf{q}_n} = \beta \mathbf{q}_n$ and $\hat{\mathbf{p}_n} = \beta^{-1}\mathbf{p}_n$, Eq. (10) becomes

$$\hat{\mathbf{p}_n}^2 + \left(1 - \beta\frac{(\omega h)^2}{4}\right)\beta^{-3}\omega^2\hat{\mathbf{q}_n}^2 = \text{Const}, \tag{11}$$

which yields a maximal relative error in the Hamiltonian equal to $(4 - \beta(\omega h)^2 - 4\beta^3)/(4 - \beta(\omega h)^2)$. This error behaves like $\mathcal{O}(h^6)$ for sufficiently small h, but unlike with the Störmer-Verlet method, it remains bounded as $h \to \bar{h}$, and overall improvement [4].

3.3 Simplified Takahashi-Imada Integrator

Since the matrix multiplication form of the simplified Takahashi-Imada method is same as the Takahashi-Imada method (18), they have the same stability conditions (see App. C.3).

3.4 Suzuki-Yoshida Method

The Suzuki-Yoshida method involves three iterations of the Störmer-Verlet method with different step sizes. Since $\tau_0 < \tau_1$, so long as $h < \frac{2}{h\omega\tau_1}$, then all three iterations of the Störmer-Verlet method in the scheme will be stable for the harmonic oscillator system.

4 Numerical Experiments

In this section we will apply the methods we introduced section 2 on a variety of examples of increasing complexity.

4.1 Harmonic Oscillator

We will warm up with a very simple problem regarding a harmonic oscillator moving in one direction. Taking the Hamiltonian (1) with mass $m = 1$, we will introduce a potential energy function $U(q) = \frac{1}{2}\omega^2 q^2$, where $\omega, q \in \mathbb{R}$ resulting in one degree of freedom. As initial conditions, we choose $q(0) = 0$ and $p(0) = 1$, and the parameter $\omega = 2$.

Implementation of all the methods is simple, with the derivative of the force for the Takahashi-Imada method being $f'(q) = -\omega^2$. The trajectory plots of all methods through time are the same (see Fig. 2), and we can investigate the change in energy to see how accurately the methods perform. Plots in Fig. 3 show that for this setup with $h = 0.2$, the energy levels of all methods behave very similarly over time, with the Yoshida method having the smallest magnitude, followed by the Verlet method.

To compare the methods throughout this section, we will use a plot for maximum difference in energy over some time T ($T = 10$ for this problem) as a function of step size h in loglog scale, to compare the performance of the methods with powers of the step size h.

The plot in Fig. 1 shows that the performance of the methods is as expected - Yoshida method is of fourth order while the other methods are of order two. The lines for T-I methods are overlaying which means they perform the same.

4.2 Unsymmetric Pendulum

We will consider a one dimensional case of a pendulum with a small perturbation in the potential of (1) added to destroy symmetry $U(q) = U(-q)$, as suggested in [4]. With mass $m = 1$, the potential will be $U(q) = -\cos(q) + 0.2\sin(2q)$. We set are initial conditions as $q(0) = 0$, $p(0) = 2.5$, so that the $p(t)$

remains positive and the pendulum turns round, and hence the symmetry in p will not have influence on the (numerical) solution.

For this example, it is easy to implement all of the methods because of the problem's low dimensionality and the easy computation of the derivative and Hessian of the potential. Since the simplified T-I method should be symplectic for one degree of freedom problems, we can also investigate whether this is the case.

On the maximum energy difference plot Fig. 4, we can see the comparison of the methods. The Yoshida method is behaving as expected, being of order $\mathcal{O}(h^4)$. From the second order methods, both T-I methods show the same result (hence only one of them is visible on the plot), but they are outperformed by the Verlet method. In Fig. 6 we see that for fairly small step size $h = 0.05$, the energy drift of all methods is similar. However, it was shown in [4] that using the truncated modified Hamiltonian $H(q_n, p_n) + h^2 H_3(q, p)$, the simplified T-I integrator is not symplectic in this problem, although it has only one degree of freedom. It was suggested that symplecticity alone does not guarantee a good energy conservation in the long time, since the solution must remain in a compact set. In this problem, q represents an angle of the pendulum modulo 2π, so the phase space is either a cylinder, or when not taking the periodicity into account, the Euclidean plane. In the latter case, the angle grows linearly in time, so the solution does not remain in a compact set, see Fig. 5.

4.3 Single Spring Pendulum System

Consider the single spring pendulum system, the position of the mass as a vector $\mathbf{q} = [q_x, q_y] \in \mathbb{R}^2$, with its associated momentum $\mathbf{p} \in \mathbb{R}^2$. The potential function in the Hamiltonian (1) is $U(\mathbf{q}) = V_{spring}(\mathbf{0}, \mathbf{q}) + V_{gravity}(\mathbf{q})$, where the potential energy is made up of two terms, the spring term connecting the mass to the origin $V_{spring}(\mathbf{u}, \mathbf{v}) = k_0(||\mathbf{u} - \mathbf{v}|| - r_0)^2/2$, and gravity pulling it down $V_{gravity} = gq_y$. The parameter g is the gravitational strength, k_0 is the spring force constant, and the rest length r_0 is the distance at which the energy term is minimized. Setting $g = 1$, $k_0 = 1$ and $r_0 = 1$ in the numerical simulation, we will implement all four methods to discuss the change in the energy of this system over time. The maximum energy difference over the trajectory of each numerical method also will be compared and discussed in the numerical simulation.

Suppose the time range is $T \in [0, 25]$, the step size $h = 0.005$, from Fig 8, as expected, the energy of each method changes periodically, whereas the exact solution to Hamiltonian's equations should preserve energy. We also simulate the system using different step sizes, and for each step size we compute the maximum deviation in the Hamiltonian in Fig 7 (left). Considering the time range $T \in [0, 10]$, the step size $h \in [10^{-2.5}, 10^{-1.5}]$, the initial momentum $p_0 = (0, -1)$ and position $q_0 = (1, 0)$, Fig 7 (left) shows that the maximum energy differences of the T-I method, simplified T-I method and Verlet method are $\mathcal{O}(h^2)$ and the fourth order Yoshida method is $\mathcal{O}(h^4)$.

4.4 Double Spring Pendulum System

Extending the single spring pendulum system to include a second particle, it becomes the double spring pendulum system. The new potential is $U(q) = V_{spring1}(\mathbf{0}, \mathbf{q}_1) + V_{spring2}(\mathbf{q}_1, \mathbf{q}_2) + V_{gravity}(\mathbf{q}_1) + V_{gravity}(\mathbf{q}_2)$ where $V_{spring1}(\mathbf{u}, \mathbf{v}) = k_1(||\mathbf{u} - \mathbf{v}|| - r_1)^2/2, V_{spring2}(\mathbf{u}, \mathbf{v}) = k_2(||\mathbf{u} - \mathbf{v}|| - r_2)^2/2$ and $V_{gravity}(\mathbf{q}) = gq_y$. The coefficients have the same meaning as in the single spring pendulum problem.

As in the previous sections, we simulate the behaviour of the energy changing in this system applying all four methods (Fig 9). Suppose the spring force constants of each spring are the same $k_1 = k_2 = 1$ and the rest lengths of both springs are $r_1 = r_2 = 1$, the initial position of each spring $\mathbf{q}_1 = (-0.1, -0.9)$, $\mathbf{q}_2 = (-0.25, -1.5)$ and the initial momentum are $\mathbf{p}_1 = (0.1, 0.2)$ and $\mathbf{p}_2 = (0.3, 0.4)$. In Fig. 9, we observe that the energy of each method also changes periodically in time range $T \in (0, 10)$. The max energy difference can be seen in Fig 7 (right), where the initial value of the positions of these two springs

are $\mathbf{q}_1 = (1, 1)$ and $\mathbf{q}_2 = (1, 0)$, the initial momenta are $\mathbf{p}_1 = (0, -1)$ and $\mathbf{p}_2 = (0, -1)$, the end time point $T = 10$. Compared to the single spring pendulum model, the simplified T-I integrator now performs similarly to the Verlet method. The Yoshida method is less accurate than in the previous model, and out of the all methods, the T-I integrator has the worst accuracy with respect to energy conservation, just like in the single spring pendulum case.

4.5 Trimer Model

We will now simulate the trimer model in vacuum with three atoms moving in the plane. They are bounded by the Lennard-Jones potential in a simple parameter setting $\phi_{LJ}(r) = r^{-12} - r^{-6}$ for interatomic distance $r = \|\mathbf{q}_i - \mathbf{q}_j\|_2$ with $\mathbf{q}_i = [q_{i,x}, q_{i,y}]$. The total potential energy of this model is $U_{LJ} = \sum_{i=1}^{2} \sum_{j=i+1}^{3} \Phi_{LJ}(\|\mathbf{q}_i - \mathbf{q}_j\|)$. The motion of the atoms is chaotic and confined by the energy.

Initially we place the atoms on the vertices of an equilateral triangle, where the distance of the atoms (length of the sides) is the minimiser of ϕ_{LJ}, $\min_{LJ} = 2^{1/6}$. The initial momentum is set to be a random vector. Because we are modelling in two dimensions, the position and momentum vectors containing all three atoms will be 6-dimensional, $\mathbf{q}, \mathbf{p} \in \mathbb{R}^6$, with $\mathbf{q} = (\mathbf{q}_1, \mathbf{q}_2, \mathbf{q}_3)$.

In order to use the T-I method, we need to compute the gradient and Hessian of the potential, where the Hessian will be a 6×6 matrix, since we must take derivatives with respect to each component of each atom. The other methods (simplified T-I, Verlet, and Yoshida) are implemented more easily.

There is no noticeable difference in the trajectories of the atoms computed by all the methods we consider, so we will focus on their energy conservation by inspecting the maximum difference plot in Fig. 10. Compared to the unsymmetric pendulum example, Yoshida method performs slightly worse. Out of the second order methods, the T-I method seems to get worse after $h > 0.03$. The Verlet method seems to perform better than the simplified T-I method. In Fig. 11, we see that for $h = 0.01$, the oscillations in energy of the Verlet and the simplified T-I method are similar in the oscillations and in magnitude. The energy growth trend of the T-I integrator over the time shown is not clear, but may be decreasing.

4.6 12-Atom System

We consider a model of 12 particles placed along the perimeter of a unit circle with non-zero, random momentum as seen in Fig. 12. After we define the positions of these atoms, we can create a vector of initial positions $\mathbf{q}_0 \in \mathbb{R}^{24}$. To set up the terms by which the particles will interact, we will introduce a potential function $U(\mathbf{q}) = U_{LJ}(\mathbf{q}) + U_{spring}(\mathbf{q})$ to the Hamiltonian system (1), with the Lennard-Jones potential energy

$$U_{LJ} = \sum_{i=1}^{N-1} \sum_{j=i+1}^{N} \Phi_{LJ}(\|\mathbf{q}_i - \mathbf{q}_j\|) = \sum_{i=1}^{N-1} \sum_{j=i+1}^{N} \alpha \left[\left(\frac{\sigma}{r_{ij}} \right)^{12} - \left(\frac{\sigma}{r_{ij}} \right)^{6} \right],$$

$r_{ij} = \|\mathbf{q}_i - \mathbf{q}_j\|$, and each atom will be attached to the origin by a length bond treated as a spring with potential energy

$$U_{spring} = \sum_{i=1}^{N} \Phi_{spring}(\|\mathbf{q}_i\|) = \sum_{i=1}^{N} \frac{k}{2}(r_i - r_0)^2,$$

where $r_i = \|\mathbf{q}_i\|$ and $\mathbf{q}_i = [q_{i,x}, q_{i,y}]$. Details about the choice of coefficients and their meaning can be found in Appendix B.

For this problem, implementing the Takahashi-Imada method would mean to compute a 24×24 Hessian of the potential, so we omitted this method. Instead, we take into consideration the first order symplectic Euler's method to compare its performance with the higher order methods.

We simulate the maximum energy difference of each method and observe the behavior does not show similar results to the other models for our very small value of k, the spring constant, see Appendix B. As seen in Fig. 13, all the methods have significantly large energy differences, including the lower order, such as Euler and Verlet. In fact, the lowest difference for symplectic Euler and Verlet is larger by a factor of nearly 10^{32}. It is interesting to note that the simplified Takahashi-Imada and Yoshida methods exhibit some noise, not seen in previous models, with the former method having much more noise than the latter. The Yoshida method performs similarly to the Euler and Verlet methods, which is contradictory to previous models' results. Furthermore, the simplified Takahashi-Imada method performs the worst, which may be caused by its lack of symplecticity. Although all methods appear approximately horizontal, with little change for varying values of h, suggesting there is no correlation between h and energy difference, which once again contradicts previous models. We increased the value of k to several values: to $k = 18/2^{32/3}$, $k = 18/2^{27/3}$, and $k = 1$, all of which were too large to produce results and produced a computational error.

Finally, we also observe total energy of each method over time with $h = 0.01$ as seen in Fig. 14. It is most apparent that we lose the oscillations observed previously with the smaller models. However, the noise seen in the orange line of the simplified Takahashi-Imada suggests possible weak or irregular oscillations, however, the maximum energy difference plot showed that this method achieved the worst results. The other methods, Euler, Verlet and Yoshida, appear significantly different to the previous models. However, all methods appear to converge to different energy values. Euler and Verlet exhibit very similar behavior over time, and even converge to similar values, but these two methods are very different from the higher order methods over time. Based on these results, it appears as though these higher order schemes produce more noise for the energy difference plots and are harder to implement with many particle systems, suggesting the lower order schemes are better methods for such complex systems. However, the simplified Takahashi-Imada method seems to be the most promising higher-order method.

5 Discussion and Conclusion

The aim of this paper was to determine whether higher order numerical methods were worth applying to Hamiltonian systems when considering the tradeoff between their accuracy against their computational and mathematical costs. As we know, lower order methods, such as the Euler and Verlet, have lower accuracy but are computationally cheap, with the latter requiring one force evaluation. The Takahashi-Imada method makes use of second-derivative Hessians, obviously becoming more challenging to calculate or derive for more complex, higher dimensional systems. The simplified Takahashi-Imada method eliminates the need for the Hessian, thus becoming less mathematically complicated for larger systems. Finally, the Yoshida method is essentially the Verlet method iterated three times with different step sizes, resulting in three force evaluations. Hence, we can see that these higher-order methods become increasingly difficult to use as we add more and more particles to the system, as we have observed in section 4. For the single to three particle systems, we see they behave well: the analytically fourth-order Yoshida is consistently approximately fourth order in simulations and achieves the best results. However, we note that the Hessian in the Takahashi-Imada already becomes a hassle with the six-dimensional system of the trimer model, rendering it too complex for our large 12-particle system. As a result, we conclude it does not seem feasible to apply the regular Takahashi-Imada method to large systems.

Our simulations consider first the total energy computed by each method over time. For all the models except the 12 particle, we observe significant oscillations. As more particles are added to a model, the more oscillations occur. In the 12 particle model, we observe that the oscillations stop, with possible exception with the simplified Takahashi-Imada. The increase in oscillations with more particles may be due to more random behavior from the increased randomness of the particles' momentum. For almost all models, we

note that the higher order methods perform well. However, as stated previously, the Takahashi-Imada method requires complex second derivative calculations, making it less than ideal beyond a three particle system. Furthermore, since the Yoshida method is essentially the Verlet method iterated three times, it can become quite computationally expensive, especially as the number of particles increase. Thus, neither of these higher-order methods are ideal for increasing model sizes for various reasons. However, the simplified Takahashi-Imada method, though more computationally costly than Euler and Verlet, gave more consistent results for the large system.

Our simulations then considered the maximum energy difference of each method for varying step size h. We found that the maximum energy difference plots became more irregular and deviated more from the expected outcome as we increased the number of particles in the system. Beginning with the trimer model, we found that the Takahashi-Imada method was no longer order two and began to increase exponentially. As stated previously, we were unable to produce simulations for the Takahashi-Imada method in the 12 particle model. However, the simplified Takahashi-Imada method performed consistently across all models until the 12 particle system, where extreme noise was observed. It also produced greater errors than the Yoshida method in the 12 particle system. We must note that the Takahashi-Imada methods were not processed to achieve order four in this report. However, it was shown the processing a method to achieve fourth order can be done at virtually no cost [10].

Finally, we may conclude that, as expected, there is not an ideal numerical scheme that works for all models, with both high accuracy and low cost. We note that these higher-order methods may be considered valuable for certain cases and models, especially with few particles in the system, such as the pendulum examples as well as the harmonic oscillator. In particular, the Yoshida and simplified Takahashi-Imada methods are better applied to models with increasing complexity, as they performed most consistently across the models. However, the Yoshida model may prove computationally costlier, and thus less attractive, than the simplified Takahashi-Imada.

References

[1] B. Leimkuhler, C. Matthews, Molecular Dynamics: With deterministic and stochastic numerical methods, *Interdisciplinary Applied Mathematics* **39**, Springer, 2015, ISBN: 978-3-319-16375-8, doi: 10.1007/978-3-319-16375-8

[2] G. Rowlands, A numerical algorithm for Hamiltonian Systems, *J. Comput. Physics* **97**, pp. 235-239, 1991, doi: 10.1016/0021-9991(91)90046-N.

[3] M.A. López-Marcos, J.M. Sanz-Serna, R.D. Skeel, Explicit symplectic integrators using Hessian-Vector products, *SIAM J Sci. Comput.* **18**, pp. 223-238, 1997, doi: 10.1137/S1064827595288085.

[4] E. Hairer, R. McLachlan, R. Skeel, On the energy conservation of the simplified Takahashi-Imada method, *ESAIM: M2AN* **43**, pp. 631–644, 2009, doi: 10.1051/m2an/2009019.

[5] E. Hairer, C. Lubich, G. Wanner, Geometric numerical integration illustrated by the Störmer–Verlet method, *Acta Numerica* **12**, pp. 399-450, 2003, doi: 10.1017/S0962492902000144.

[6] J.C. Butcher, The effective order of Runge-Kutta methods, *Proceedings of Conference on the Numerical Solution of Differential Equations* **109**, pp. 133-139, 1969, ISBN: 978-3-540-04628-8.

[7] J. Wisdom, M. Holman, J. Touma, Symplectic Correctors, *Amer. Math. Soc. Providence R.I.* **10**, pp. 217-244, 1996. `http://web.mit.edu/wisdom/www/Symplectic_Correctors.pdf`. Accessed 19 April 2020.

[8] M. Takahashi, M. Imada, Monte Carlo calculation of quantum systems. II. Higher order correction, *J Phys Soc Jpn* **53**, pp. 3765–3769, 1984, doi: 10.1143/JPSJ.53.3765.

[9] L. Wang-Yao, On stability of symplectic algorithms, *J. Comp. Math* **13**, pp. 64-69, 1995. *JSTOR*, `www.jstor.org/stable/43692603`. Accessed 16 April 2020.

[10] M.A. López-Marcos, J.M. Sanz-Serna, R.D. Skeel, An explicit symplectic integrator with maximal stability interval, *Numerical Analysis*, pp. 163-175, 1996, doi: 10.1142/9789812812872_0012

[11] GitHub repository for the code: `https://github.com/KarolinaBenkova/group6-repo.git`

Appendix A Figures

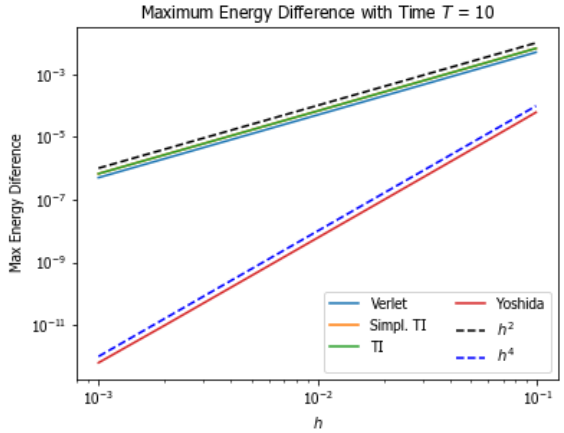

Figure 1: Harmonic oscillator: the max. energy difference as a function of h over time $T = 10$.

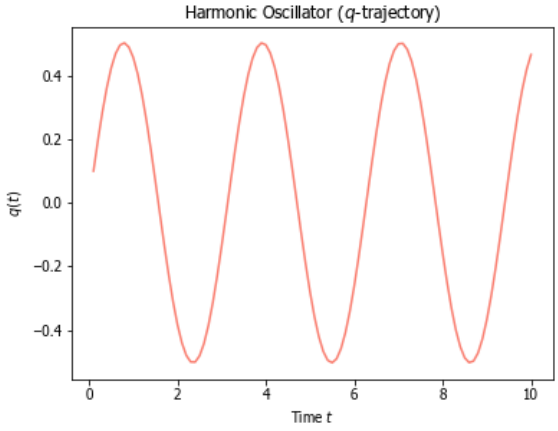

Figure 2: Harmonic oscillator: trajectory of q over time using the Verlet method and $h = 0.1$

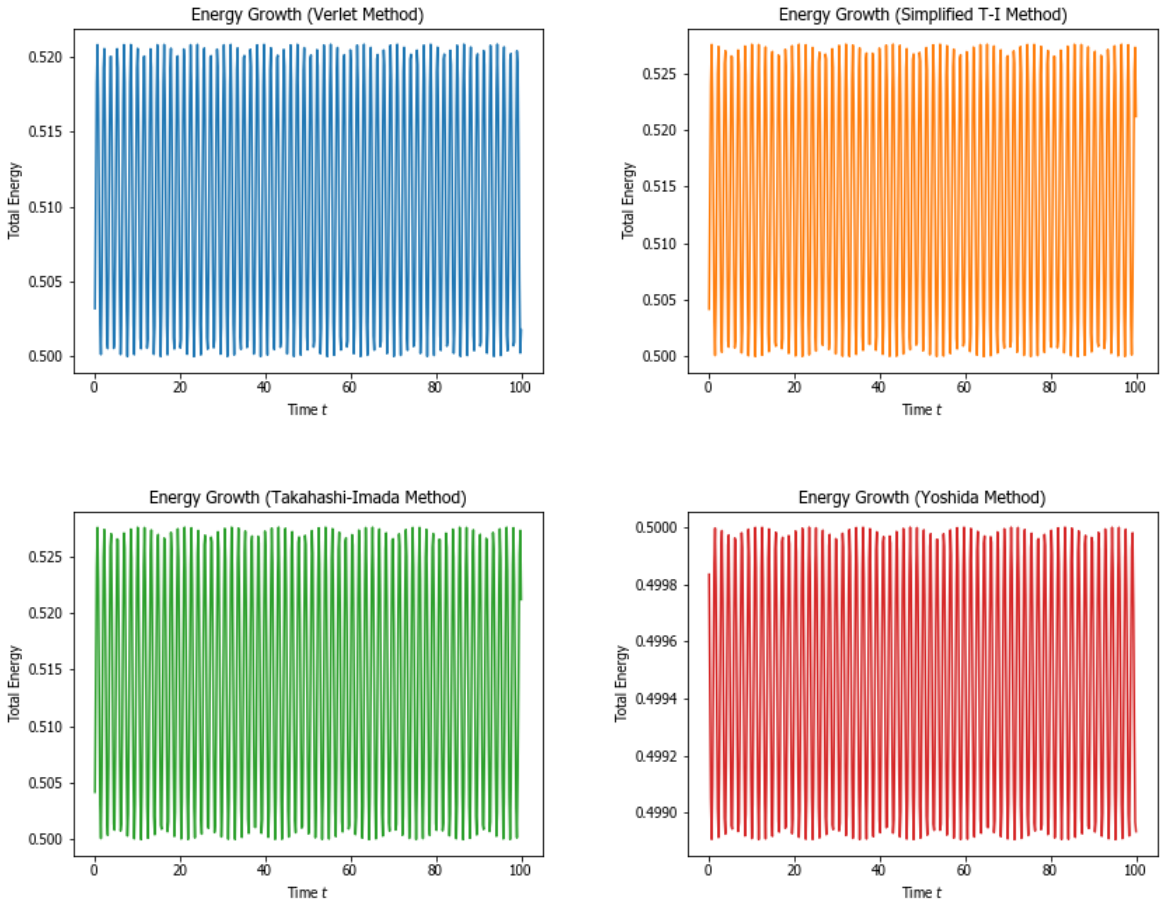

Figure 3: Harmonic oscillator: the energy growth of the methods with $h = 0.2$. The true energy is $H(q_0, p_0) = 0.5$.

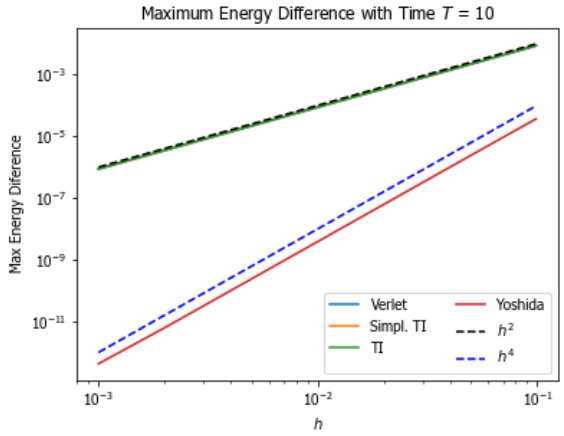

Figure 4: Unsymmetric pendulum: the max. energy difference as a function of h over time $T = 10$.

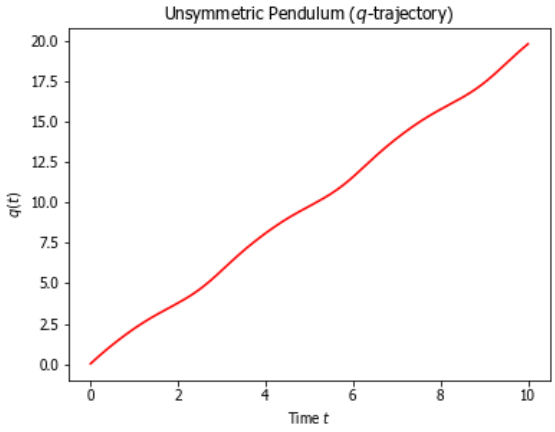

Figure 5: Unsymmetric pendulum: trajectory of q over time using the Verlet method and $h = 0.01$.

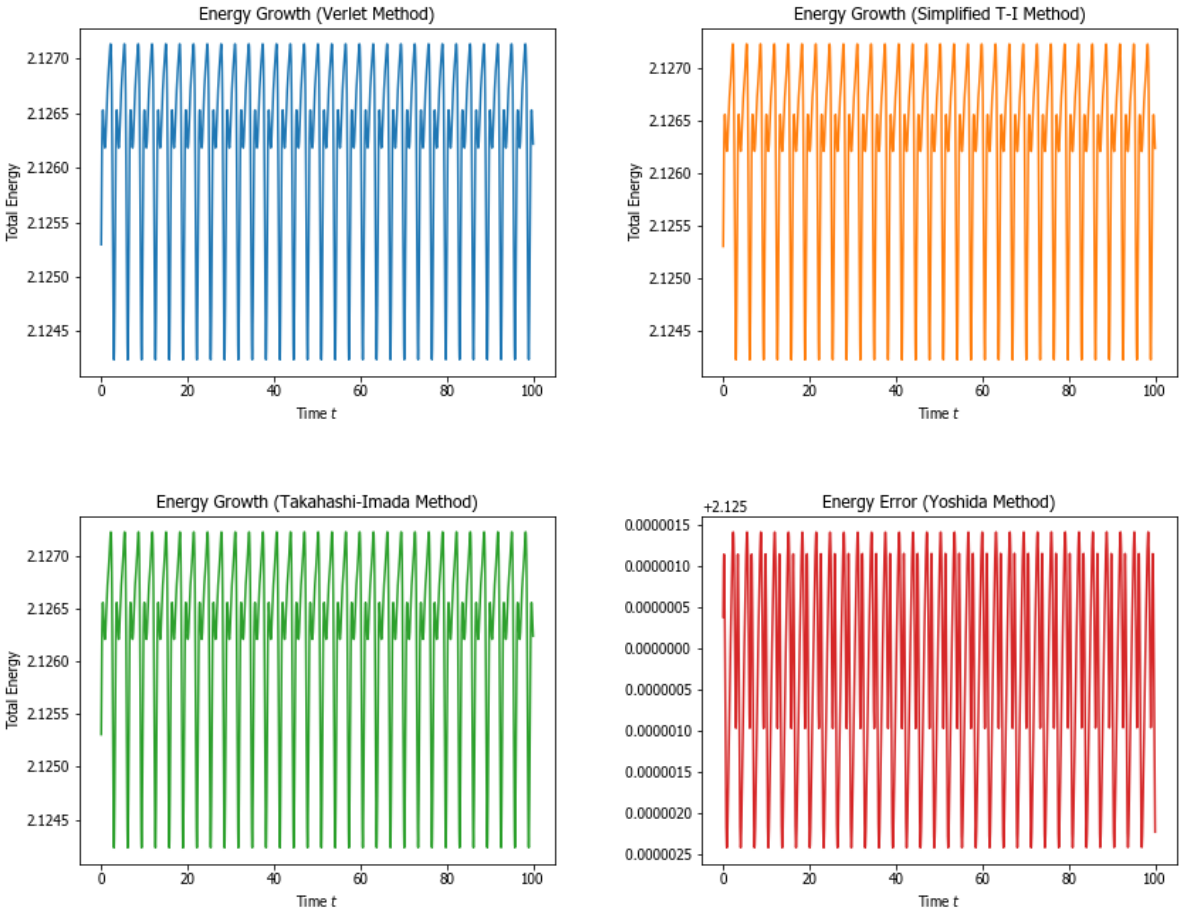

Figure 6: Unsymmetric pendulum: the energy growth of the methods with $h = 0.05$. The true energy is $H(q_0, p_0) = 2.125$.

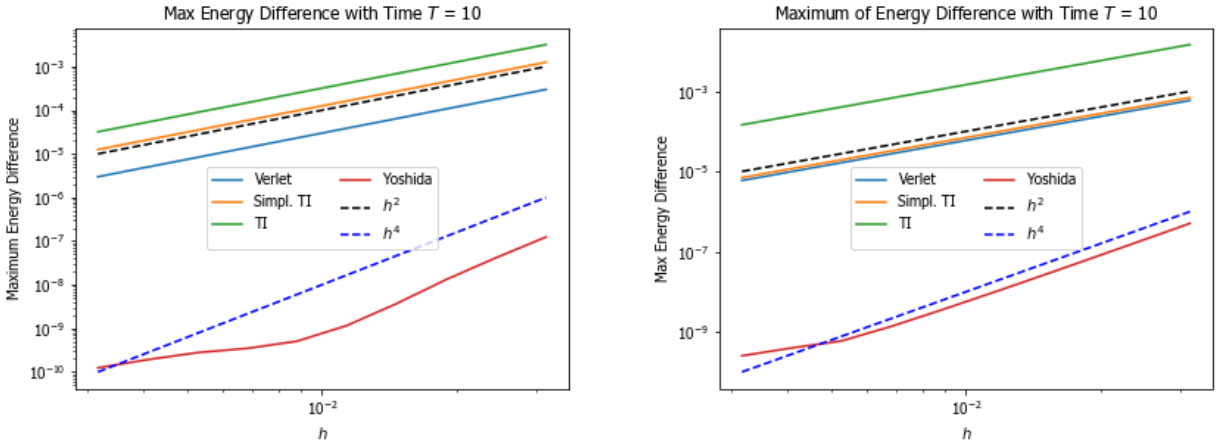

Figure 7: The spring pendulum model: the maximum energy difference. On the left, single pendulum system; on the right, double pendulum.

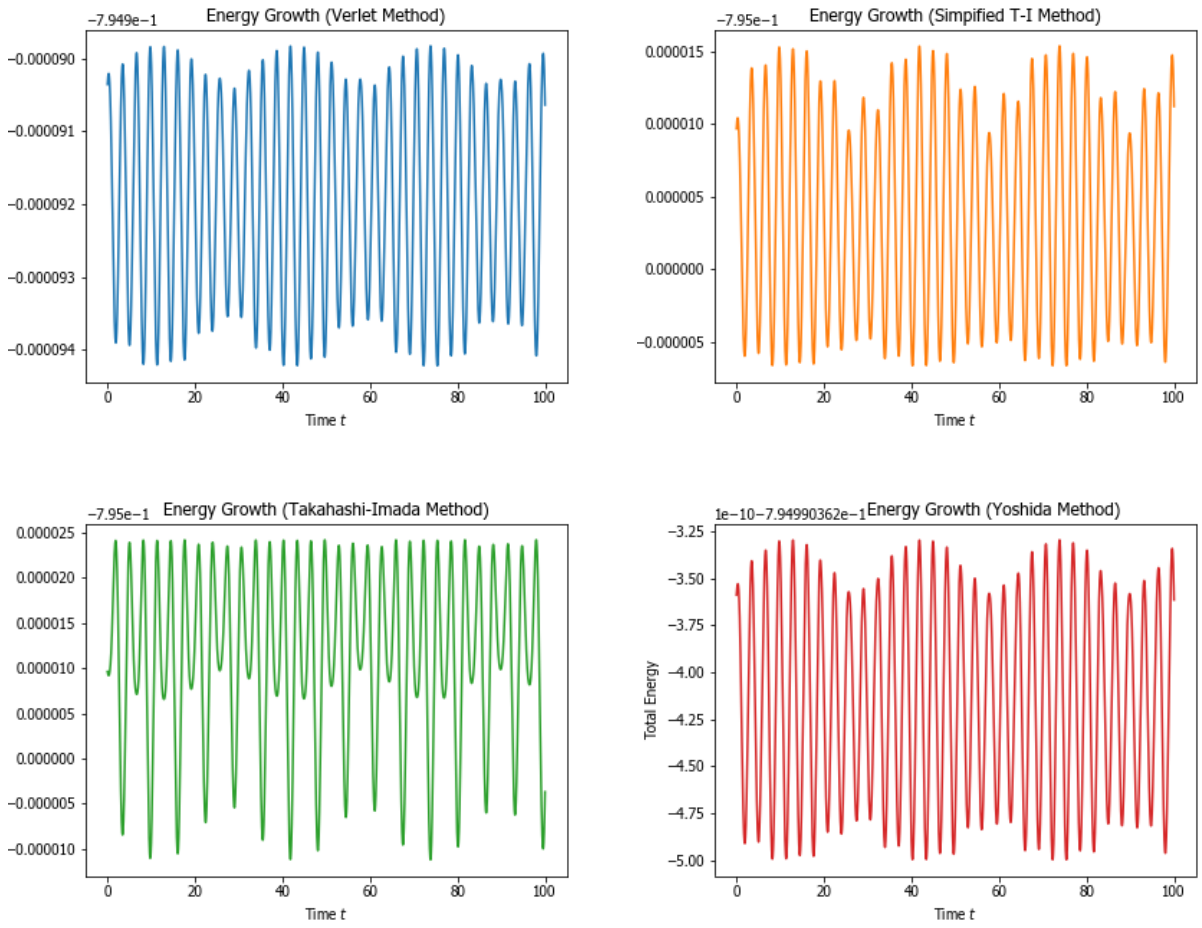

Figure 8: Single spring pendulum: the energy growth of the methods with $h = 0.005$. The true energy is $H(q_0, p_0) = -0.795$.

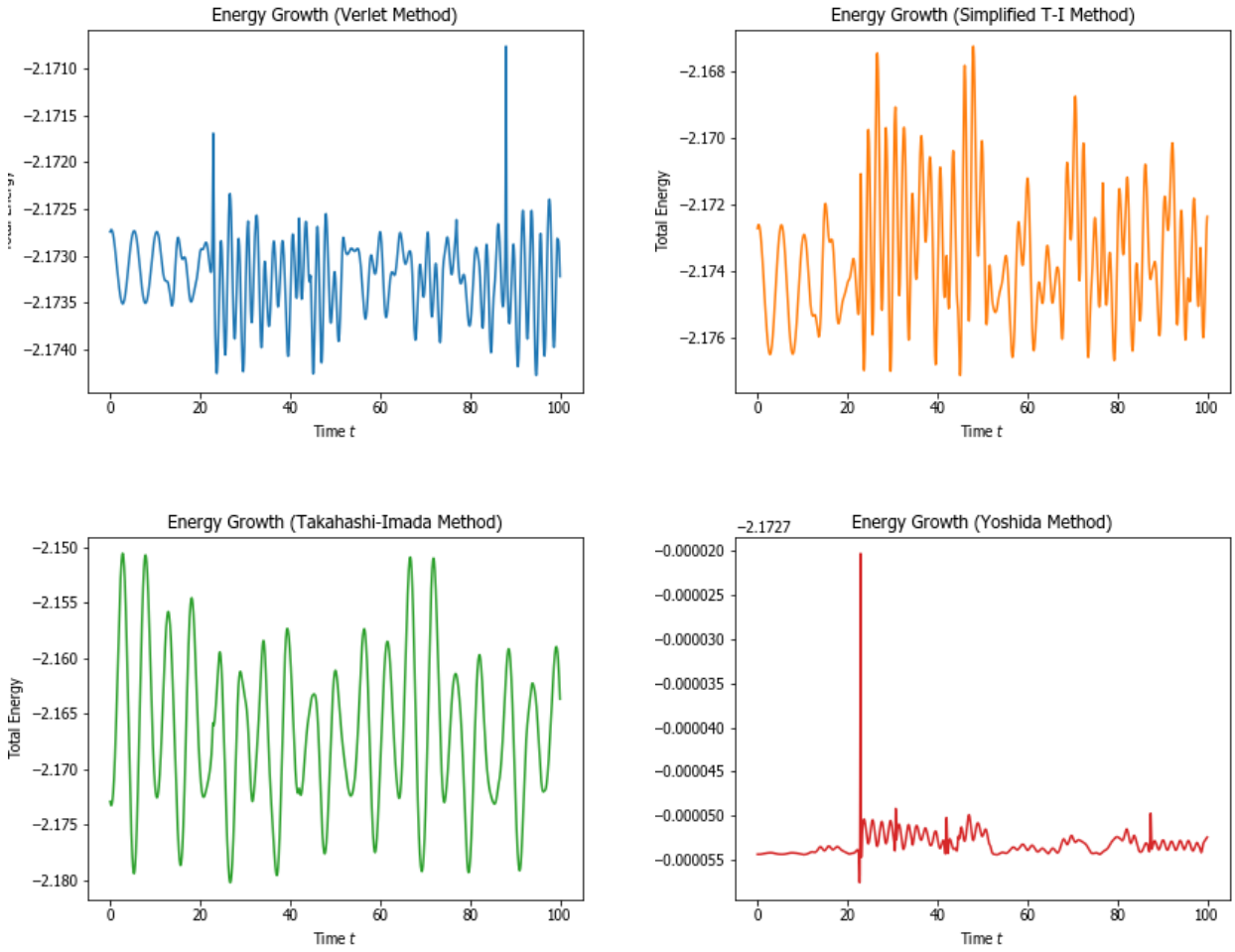

Figure 9: Double spring pendulum: the energy growth of the methods with $h = 0.05$. The true energy is $H(q_0, p_0) = -2.173$.

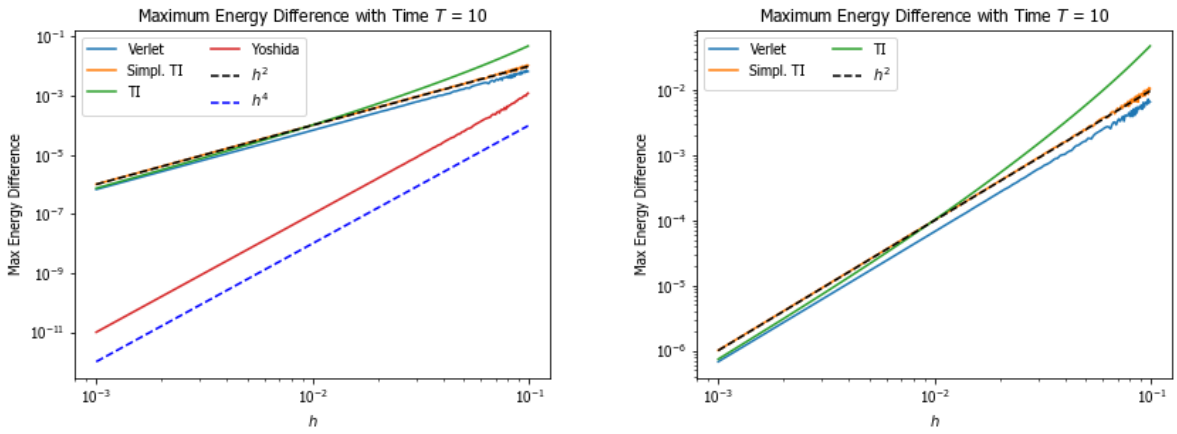

Figure 10: The trimer model: the maximum energy difference as a function of step size h over time $T = 10$. On the left, all methods, on the right, detail on the second order methods.

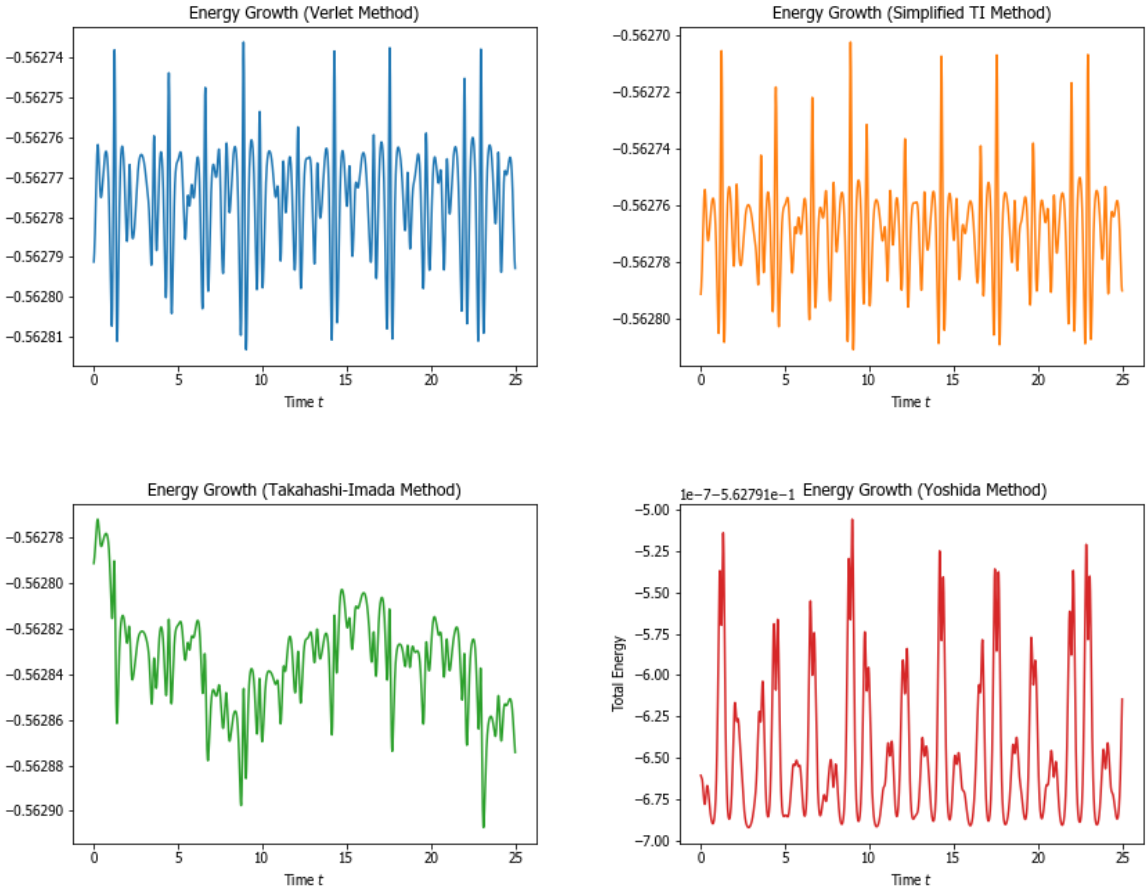

Figure 11: The trimer model: the energy growth of the methods with $h = 0.01$. The true energy is $H(q_0, p_0) = -0.606$.

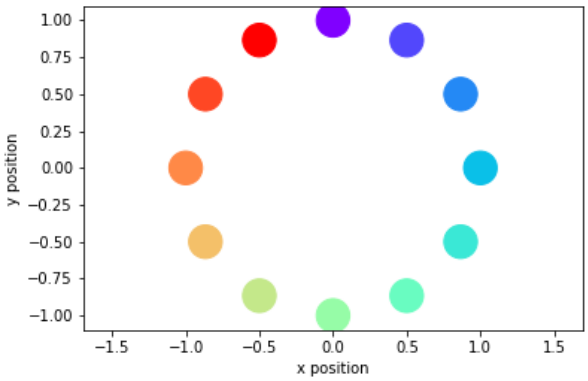

Figure 12: 12-particle model: The initial positions of the 12 particles.

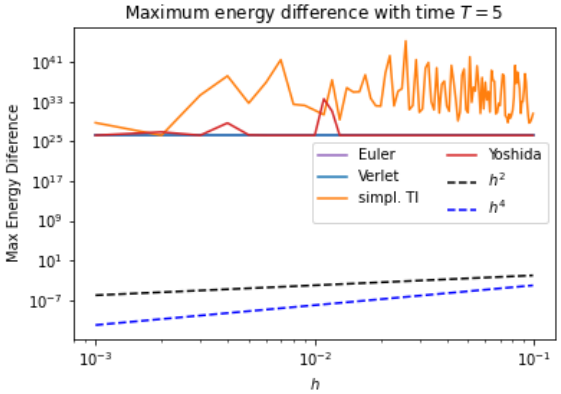

Figure 13: The 12 particle model: the maximum energy difference as a function of step size h over time $T = 10$.

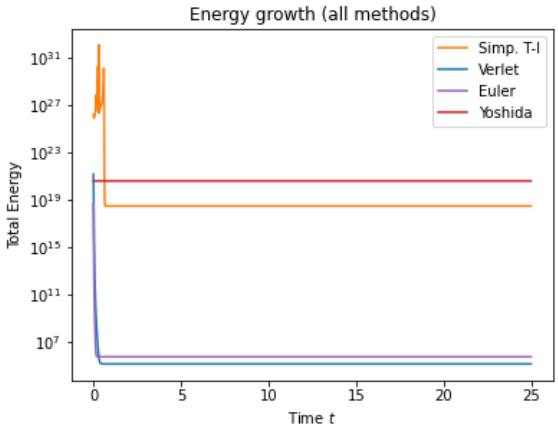

Figure 14: The 12 particle model: the total energy growth over time with $h = 0.01$ and $T = 25$. The true energy is $H(q_0, p_0) = 1.53 \times 10^{26}$.

Appendix B Coefficients of the 12-Atom Model

Firstly, we compute the stationary point $r = r^*$ of the Lennard-Jones potential:

$$\frac{d\Phi_{LJ}}{dr} = 0 \iff r = 2^{1/6}\sigma = r^*.$$

Then we evaluate the second derivative at $r = r^*$

$$\frac{d^2\Phi_{LJ}}{dr^2}|_{r=r^*} = \alpha\left(156\frac{\sigma^{12}}{r^{14}} - 42\frac{\sigma^6}{r^8}\right)|_{r=r^*} = \alpha\left(\frac{39}{2^{1/3}\sigma^2} - \frac{21}{2^{1/3}\sigma^2}\right) = \frac{18\alpha}{2^{1/3}\sigma^2}.$$

The resulting value is positive, $\frac{d^2\Phi_{LJ}}{dr^2}(r^*) > 0$, which means that the stationary point is a local minimum, where the potential energy has a stable equilibrium (for $\alpha > 0$).

We will expand U_{LJ} in Taylor series up to the second order around r^*:

$$\Phi_{LJ}(r) = \Phi_{LJ}(r^*) + \frac{1}{2}\frac{d^2\Phi_{LJ}}{dr^2}(r^*)(r-r^*)^2 + ... = -\frac{3}{4}\alpha + \frac{1}{2}\frac{18\alpha}{2^{1/3}\sigma^2}(r - 2^{1/6}\sigma)^2 + ...$$

and compare this approximation to $\Phi_{spring}(q) = \frac{1}{2}k(r-r_0)^2$ to choose a value of the parameter k. We see that they have a similar structure up to the constant $\Phi_{LJ}(r^*)$ and hence we can compare k to $\frac{d^2\Phi_{LJ}}{dr^2}(r^*)$, setting $\sigma = 2^6$ so that $r^* = r_0 = 1$ because of the unit circle configuration. We decide to choose $\alpha = 1$ for simplicity, and $k = \frac{18}{2^{37/3}}$.

Appendix C Harmonic Oscillator Stability Derivations

The Hamiltonian for the harmonic oscillator system we considered in Section 4 is:

$$H(\mathbf{q},\, \mathbf{p}) = \frac{1}{2}\mathbf{p}^\top\mathbf{M}^{-1}\mathbf{p} + \frac{1}{2}\omega^2\mathbf{q}^2 \tag{12}$$

To simplify our calculations, we set $\mathbf{M} = \mathbf{I}$. Below are the derivations for the eigenvalues we used in our stability analysis for each numerical method:

C.1 Störmer-Verlet Method

When we substitute the Hamiltonian (Eq. (12)) into the numeric scheme (Eq. (5)), we arrive at

$$\begin{aligned}
\mathbf{p}_{n+\frac{1}{2}} &= \mathbf{p}_n - \frac{h}{2}\omega^2\mathbf{q}_n, \\
\mathbf{q}_{n+1} &= h\mathbf{p}_n + \left(1 - \frac{h^2\omega^2}{2}\right)\mathbf{q}_n, \\
\mathbf{p}_{n+1} &= \left(1 - \frac{h^2\omega^2}{2}\right)\mathbf{p}_n - h\omega^2\left(1 - \frac{h^2\omega^2}{4}\right)\mathbf{q}_n.
\end{aligned} \tag{13}$$

The system for $\begin{bmatrix}\mathbf{q}_{n+1}\\ \mathbf{p}_{n+1}\end{bmatrix}$ in matrix multiplication form is

$$\begin{bmatrix}\mathbf{q}_{n+1}\\ \mathbf{p}_{n+1}\end{bmatrix} = \begin{bmatrix} 1 - \frac{h^2\omega^2}{2} & h \\ -h\omega^2\left(1 - \frac{h^2\omega^2}{4}\right) & 1 - \frac{h^2\omega^2}{2}\end{bmatrix}\begin{bmatrix}\mathbf{q}_n\\ \mathbf{p}_n\end{bmatrix}. \tag{14}$$

The eigenvalues of the matrix are

$$\lambda_{1,2} = 1 - \frac{h^2\omega^2}{2} \pm \frac{h^2\omega^2}{2}\sqrt{1 - \frac{4}{h^2\omega^2}}. \tag{15}$$

Whenever $h^2\omega^2 < 4$, the eigenvalues are imaginary. This is occurs for a step size $h > 0$ where $h < \frac{2}{\omega}$. In this case, we can represent Eq. (15) as

$$\lambda_{1,2} = 1 - \frac{h^2\omega^2}{2} \pm i\frac{h^2\omega^2}{2}\sqrt{\frac{4}{h^2\omega^2} - 1}. \tag{16}$$

These eigenvalues have the following magnitude

$$\|\lambda_{1,2}\| = \left(1 - \frac{h^2\omega^2}{2}\right)^2 + \frac{h^4\omega^4}{4}\left(\frac{4}{h^2\omega^2} - 1\right) = 1 + \left(h^2\omega^2 - h^2\omega^2\right) + \left(\frac{h^4\omega^4}{4} - \frac{h^4\omega^4}{4}\right) = 1. \tag{17}$$

Since the eigenvalues are imaginary and their magnitude is 1, they reside on the unit circle in the complex plane.

C.2 Takahashi-Imada Integrator

Since $\nabla^2 U(\mathbf{q}) = \nabla^2\left(\frac{1}{2}\omega^2\mathbf{q}^2\right) = \omega^2\mathbf{I}$, we can define a matrix $\mathbf{\Phi} = (\mathbf{I} - \alpha h^2\nabla^2 U(\mathbf{q})) = (\mathbf{I} - \alpha h^2\omega^2\mathbf{I}) = (1 - \alpha h^2\omega^2)\mathbf{I} = \phi\,\mathbf{I}$ to simplify our forthcoming derivations. When we substitute the Hamiltonian (Eq. (12)) into the numerical scheme (Eq. (6)), we arrive at

$$\begin{aligned}
\mathbf{q}_{n+1/2} &= \mathbf{p}_n - \frac{h\omega^2}{2}\phi\,\mathbf{q}_n \\
\mathbf{q}_{n+1} &= h\mathbf{p}_n + \left(1 - \frac{h^2\omega^2}{2}\phi\right)\mathbf{q}_n \\
\mathbf{p}_{n+1} &= \left(1 - \frac{h^2\omega^2}{2}\phi\right)\mathbf{p}_n - h\omega^2\phi\left(1 - \frac{h^2\omega^2}{4}\right)\mathbf{q}_n
\end{aligned} \tag{18}$$

The system for $\begin{bmatrix}\mathbf{q}_{n+1}\\ \mathbf{p}_{n+1}\end{bmatrix}$ in matrix multiplication form is

$$\begin{bmatrix}\mathbf{q}_{n+1}\\ \mathbf{p}_{n+1}\end{bmatrix} = \begin{bmatrix} 1 - \frac{h^2\omega^2}{2}\phi & h \\ -h\omega^2\phi\left(1 - \frac{h^2\omega^2}{4}\phi\right) & 1 - \frac{h^2\omega^2}{2}\phi \end{bmatrix}\begin{bmatrix}\mathbf{q}_n\\ \mathbf{p}_n\end{bmatrix}. \tag{19}$$

The eigenvalues of the matrix are

$$\lambda_{1,2} = 1 - \frac{h^2\omega^2}{2}\phi \pm \frac{h^2\omega^2}{2}\phi\sqrt{1 - \frac{4}{h^2\omega^2\phi}} \tag{20}$$

Whenever $h^2\omega^2\phi = h^2\omega^2\left(1 - \alpha h^2\omega^2\right) < 4$, the eigenvalues are imaginary. This is occurs with a step size $h > 0$ such $(1 - \alpha h^2\omega^2) = 0$, or $h < \frac{1}{\omega\sqrt{\alpha}}$. In this case, we can represent Eq. (20) as

$$\lambda_{1,2} = 1 - \frac{h^2\omega^2}{2}\phi \pm i\frac{h^2\omega^2}{2}\phi\sqrt{\frac{4}{h^2\omega^2\phi} - 1} \tag{21}$$

These eigenvalues have the following magnitude

$$\|\lambda_{1,2}\| = \left(1 - \frac{h^2\omega^2}{2}\phi\right)^2 + \frac{h^4\omega^4}{4}\phi^2\left(\frac{4}{h^2\omega^2\phi} - 1\right) = 1 + \left(h^2\omega^2\phi - h^2\omega^2\phi\right) + \left(\frac{h^4\omega^4}{4}\phi^2 - \frac{h^4\omega^4}{4}\phi^2\right) = 1. \tag{22}$$

C.3 Simplified Takahashi-Imada Integrator

Since $\nabla U\left(\mathbf{q} - \alpha h^2 \nabla U(\mathbf{q})\right)\big) = \omega^2\left(\mathbf{q} - \alpha h^2\omega^2\mathbf{q}\right) = \omega^2\left(1 - \alpha h^2\omega^2\right)\mathbf{q}$, we can define a constant $\phi = (1 - \alpha h^2\omega^2)$ to simplify our forthcoming derivations. When we substitute the Hamiltonian (Eq. (12)) into the numerical scheme (Eq. (7)), we arrive at

$$\begin{aligned}
\mathbf{q}_{n+1/2} &= \mathbf{p}_n - \frac{h\omega^2}{2}\phi\,\mathbf{q}_n \\
\mathbf{q}_{n+1} &= h\mathbf{p}_n + \left(1 - \frac{h^2\omega^2}{2}\phi\right)\mathbf{q}_n \\
\mathbf{p}_{n+1} &= \left(1 - \frac{h^2\omega^2}{2}\phi\right)\mathbf{p}_n - h\omega^2\phi\left(1 - \frac{h^2\omega^2}{4}\right)\mathbf{q}_n
\end{aligned} \tag{23}$$

Note that this system is identical to that from App. C.2. This means the eigenvalues are found in Eq. (20), and both the Takahashi-Imada Integrator and the simplified Takahashi-Imada Integrator have the same stability with regards to the simple harmonic oscillator system.

Appendix D Code

The code used to produce the plots in this report can be accessed at [11]. Our different numerical experiments can be found in separate Python notebooks in the repository.